

Supplementary Data

Selective alanine transporter utilization creates a targetable metabolic niche in pancreatic cancer

Seth J. Parker^{1,2}, Caroline R. Amendola^{2*}, Kate E. R. Hollinshead^{1,2*}, Qijia Yu^{3*}, Keisuke Yamamoto^{1,2}, Joel Encarnación-Rosado^{1,2}, Rebecca E. Rose⁴, Madeleine M. LaRue², Albert S. W. Sohn^{1,2}, Doug E. Biancur^{1,2}, Joao A. Paulo⁵, Steven P. Gygi⁵, Drew R. Jones⁴, Huamin Wang⁶, Mark R. Philips², Dafna Bar-Sagi^{2,4,7}, Joseph D. Mancias³, and Alec C. Kimmelman^{1,2#}

¹Department of Radiation Oncology, New York University School of Medicine, New York, NY.

²Perlmutter Cancer Center, New York University School of Medicine, New York, NY.

³Division of Genomic Stability and DNA Repair, Department of Radiation Oncology, Dana-Farber Cancer Institute, Boston, MA.

⁴Department of Biochemistry and Molecular Pharmacology, New York University School of Medicine, New York, NY.

⁵Department of Cell Biology, Harvard Medical School, Boston, MA.

⁶Department of Anatomical Pathology, University of Texas M.D. Anderson Cancer Center, Houston, TX.

⁷Department of Medicine, New York University School of Medicine, New York, NY.

* equal contribution (by alphabetical)

#Corresponding author: Alec C. Kimmelman, M.D., Ph.D.; Perlmutter Cancer Center, Department of Radiation Oncology, NYU Medical School, New York, NY 10016; V: (646) 501-8940; alec.kimmelman@nyulangone.org.

Content:

Supplementary Methods

Supplementary Figures S1-S11 with Legends

Supplementary Table S1

Supplementary Methods

Cell Culture

Cells were routinely maintained in DMEM (Corning) supplemented with 10% FBS (Atlanta Biologicals S11550H, Lot No. C18030) and 1% Pen/Strep (Gibco). HPDE cells were maintained in defined keratinocyte SFM (ThermoFisher) media supplemented with provided growth supplement.

Tumor Preparation for Immunohistochemistry

Tumors resected from mice were fixed in five volumes of formalin at 4°C for two days with gentle agitation and two formalin changes. Mice were not fasted prior to euthanasia and surgical resection. Tumors were washed overnight with five volumes of 70% ethanol at 4°C with gentle agitation and two ethanol changes before imaging, processing, embedding, and sectioning. Immunohistochemistry was performed on 5 µm sections.

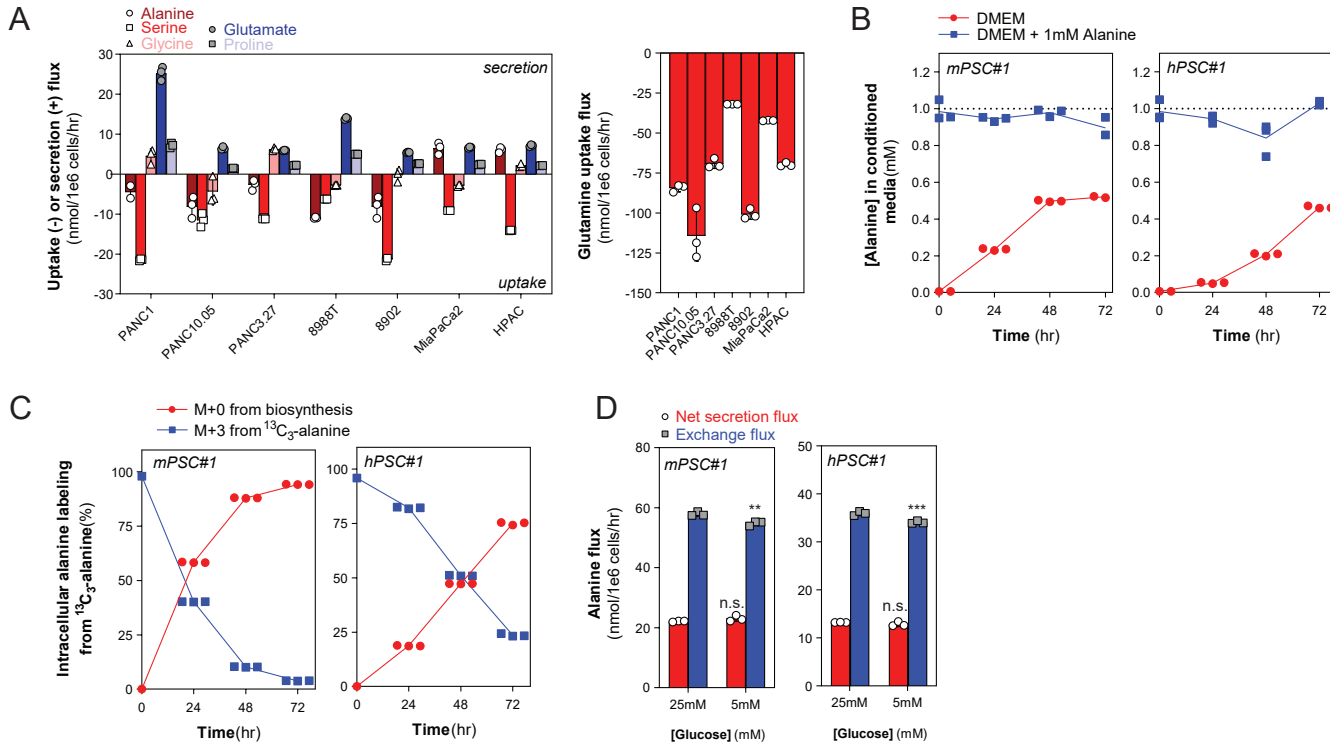
Polar and non-polar derivatization and GC-MS analysis

Polar metabolites were derivatized to form methoxime ester tert-butyl dimethyl silyl derivatives and lipids were transesterified to form fatty acid methyl esters. Briefly, to derivatize polar metabolites, 20 µl of methoxyamine hydrochloride solution (20 mg/ml, in pyridine; prepared fresh) was added to each vial and incubated at 37°C for 30-60 minutes followed by addition of 20 µl MTBSTA + 1% TBDMSCI (Sigma) and incubated for 37°C for 5-30 minutes. For non-polar derivatization, 500 µl of 2% H₂SO₄ in HPLC-grade methanol was added to each sample and incubated at 50°C for 60 minutes followed by addition of 200 µl saturated NaCl solution (in HPLC-grade water) and 500 µl of HPLC-grade hexane. Samples were centrifuged, and 300 µl of hexane layer was transferred to glass vial inserts (Agilent) for GC-MS analysis. Derivatized samples were analyzed by GC-MS using a DB-35MS or DB-5MS column (30 m x 0.25 mm i.d. x 0.25 µm) installed in an Agilent 5977B gas chromatograph (GC) interfaced with an Agilent 5977B mass spectrometer (MS). The GC temperature was held at 100°C after injection, ramped to 255°C at 7.5°C/min, ramped to 320°C at 15°C/min, held at 320°C for 3 minutes, and post-run held at 320°C for 2 additional minutes. The MS detector was operated in scan mode over a range of 100-650 m/z. Mass isotopomer distributions were determined by integrating metabolite ion fragments and corrected for natural isotope abundance using in-house algorithms.

Proliferation Assays

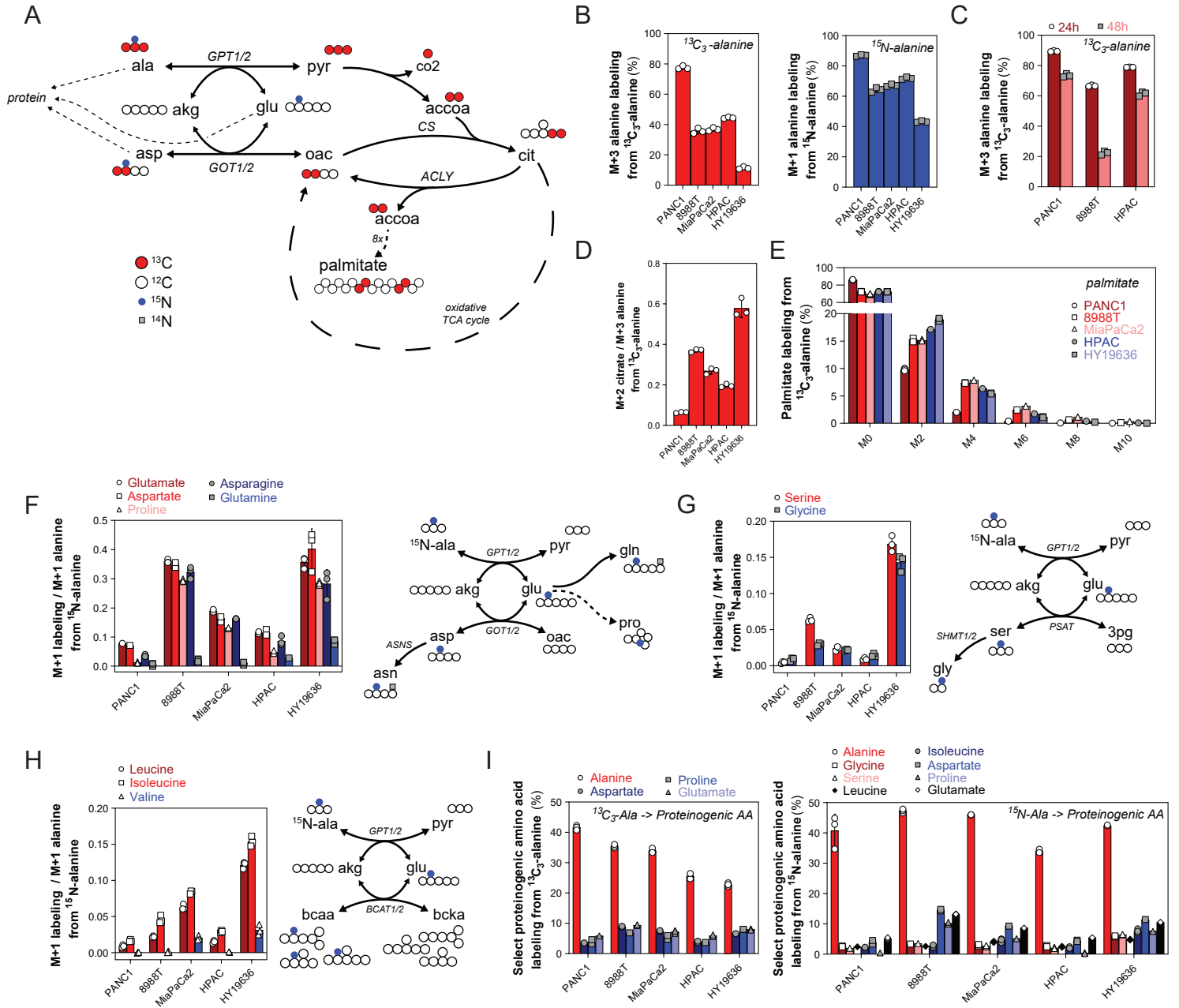
Proliferation curve time points were collected by fixing cells in 10% formalin (ThermoFisher) and staining with a 0.1% crystal violet solution (Sigma) containing 10% ethanol. Dye was extracted with 10% acetic acid (Sigma) and absorbance was measured at 595 nm using a FLUOstar Omega plate reader (BMG Labtech). Absorbance was background corrected and proliferation curves were determined by normalizing to day zero measurement. Clonogenic plates were fixed and stained in a 6% glutaraldehyde and 0.5% crystal violet solution for 60 minutes.

Supplementary Figure 1



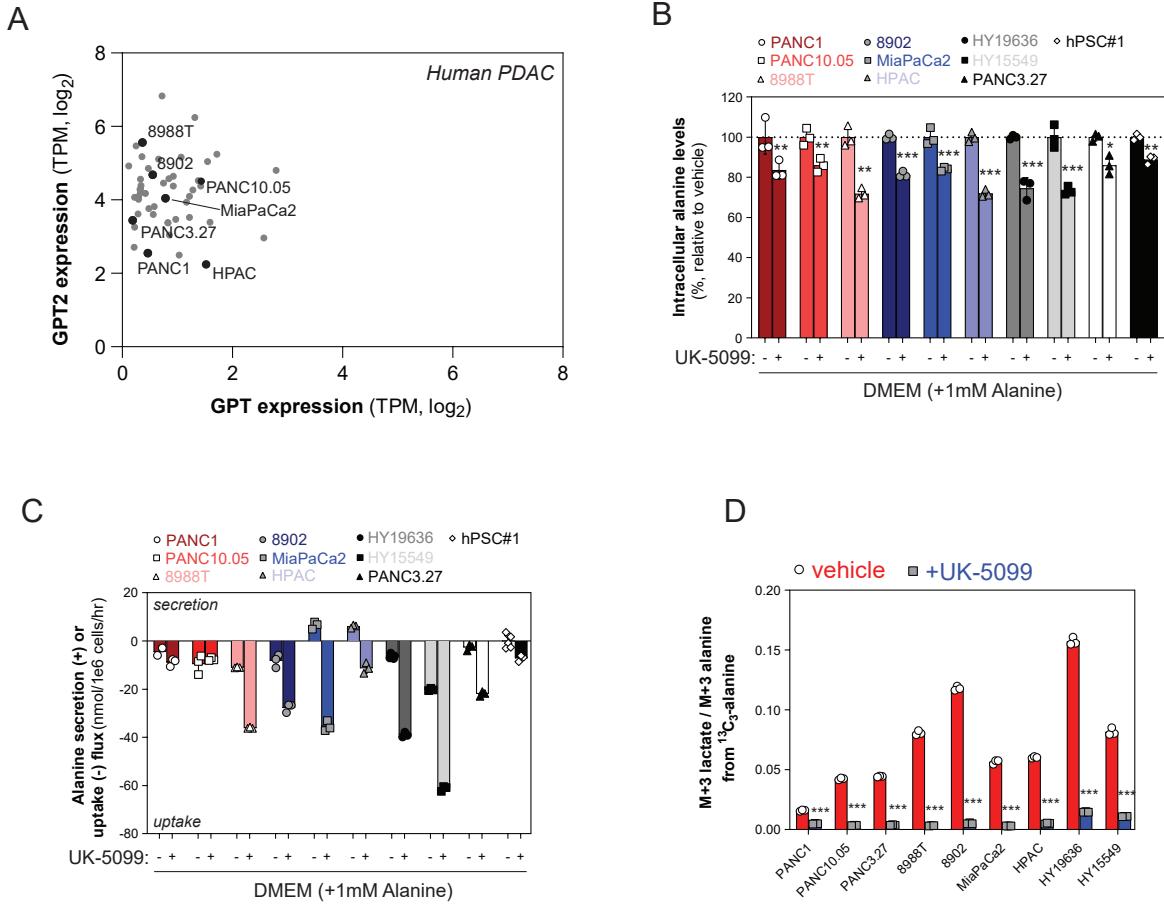
Supplementary Fig. S1. PDAC cell influx alanine and pancreatic stellate cells rapidly exchange alanine. **(A)** Alanine, serine, glycine, proline, and glutamate (*left panel*) and glutamine (*right panel*) extracellular fluxes in a panel of human PDAC cell lines cultured in DMEM. Extracellular accumulation (+, secretion) or depletion (-, uptake) was measured in conditioned media over 24-72 hours and normalized to the viable cell density over the time course. Error bars depict s.d. of three technical replicate wells normalized to cell growth of surrogate wells. Alanine data is also shown in Fig. 1A. **(B)** Extracellular alanine concentrations (in mM) in DMEM or DMEM supplemented with 1mM L-alanine conditioned by human and mouse stellate cell lines (hPSC#1, mPSC#1) over the course of 72 hours. Error bars depict s.d. of three technical replicate wells collected from independent plates for each time point. **(C)** Intracellular alanine labeling in human and mouse stellate cell lines (hPSC#1, mPSC#1) cultured in DMEM supplemented with 1mM $^{13}\text{C}_3$ -alanine over the course of 72 hours. Unlabeled (M+0) alanine increases over time, whereas uniformly ^{13}C -labeled (M+3) alanine decreases over time as extracellular alanine is diluted by exchange with synthesized alanine (M+0). Error bars depict s.d. of three technical replicate wells collected from independent plates for each time point. These data are used to quantify alanine exchange flux plotted in Fig. 1B. **(D)** Alanine exchange and net secretion fluxes in hPSC#1 and mPSC#1 quantified in DMEM containing either 25mM or 5mM glucose. $^{13}\text{C}_3$ -alanine dilution was measured over 24 hours, and the molar exchange flux was quantified and normalized by viable cell density over time course. Error bars depict s.d. of three technical replicate wells normalized by growth of surrogate wells. Significance determined with two-way ANOVA using Sidak's multiple comparisons test in **D**. n.s. $p \geq 0.05$, *** $p\text{-val} < 0.001$.

Supplementary Figure 2



Supplementary Fig. S2. Heterogeneous fate of alanine-derived carbon and nitrogen in PDAC. **(A)** Atom transition map of $^{13}\text{C}_3$ -, ^{15}N - labeled alanine. $^{13}\text{C}_3$ -alanine carbon labels downstream TCA intermediates (e.g. pyruvate, citrate) and contributes carbon to *de novo* lipogenesis. ^{15}N -alanine feeds into transaminase pathways. Large, red circles depict ^{13}C atom transitions through central carbon metabolism; small, blue circles depict ^{15}N atom transitions through the transaminase network. Unlabeled (^{12}C , ^{14}N) atoms depicted as white circles. **(B)** Intracellular alanine labeling from $^{13}\text{C}_3$ -alanine (*left panel*) or ^{15}N -alanine (*right panel*) in a panel of human PDAC cell lines cultured in DMEM supplemented with 1mM L-alanine ($^{13}\text{C}_3$ - or ^{15}N -labeled) for 24 hours. Error bars depict s.d. of three technical replicate wells. **(C)** Intracellular alanine labeling from $^{13}\text{C}_3$ -alanine decreases in human PDAC cells over time, failing to reach isotopic steady state. PDAC cells were cultured in DMEM supplemented with 1mM $^{13}\text{C}_3$ -alanine for 24 or 48 hours. Error bars depict s.d. of three technical replicate wells for each time point. **(D)** Citrate M+2 labeling normalized to alanine labeling (M+3) in human PDAC cell lines cultured in DMEM supplemented with 1mM $^{13}\text{C}_3$ -alanine for 24 hours. Error bars depict s.d. of three technical replicate wells. **(E)** Palmitate labeling (M+0, M+2, M+4, etc.) in PDAC cells cultured with $^{13}\text{C}_3$ -alanine for 24 hours. Error bars depict s.d. of three technical replicate wells. **(F, G, and H)** Labeled transaminase products (M+1) normalized to intracellular alanine labeling from ^{15}N -alanine in human PDAC cell lines cultured in DMEM supplemented with 1mM ^{15}N -alanine for 24 hours and associated atom transition maps for each transaminase pathway. Error bars depict s.d. of three technical replicate wells. **(I)** Alanine carbon (*left panel*) and nitrogen (*right panel*) contribution to select proteinogenic amino acids in human PDAC cells cultured in DMEM supplemented with 1mM of either $^{13}\text{C}_3$ -alanine or ^{15}N -alanine for 24 hours. Error bars depict s.d. of three technical replicate wells.

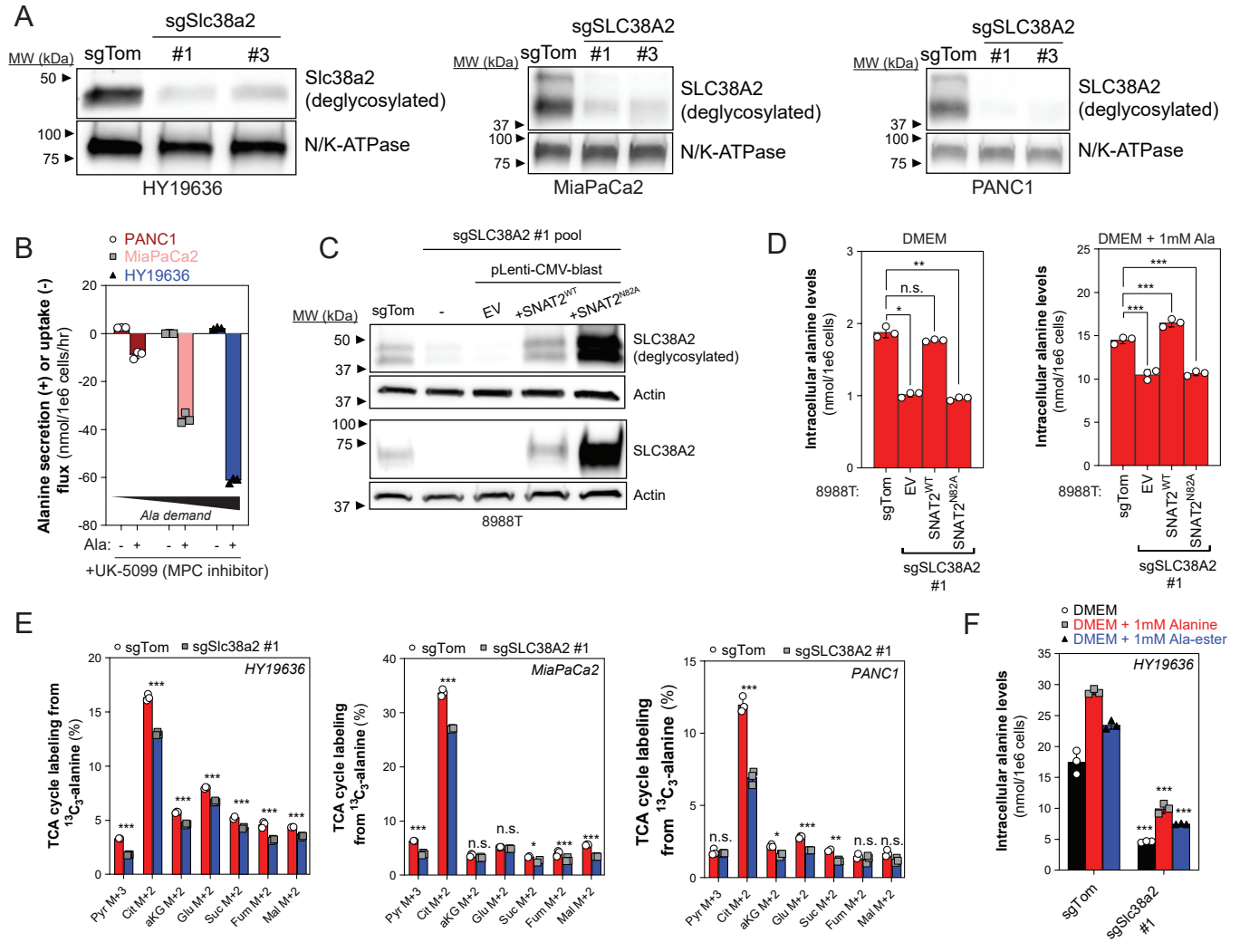
Supplementary Figure 3



Supplementary Fig. S3. PDAC cells selectively express mitochondrial GPT2 for alanine synthesis and utilization. **(A)** Relative expression of cytosolic *GPT* and mitochondrial *GPT2* in transcripts per million (TPM) in ~50 human PDAC cell lines adapted from Cancer Dependency Map (DepMap). **(B)** Intracellular alanine levels normalized by cell number in panel of PDAC cell lines and hPSC#1 in response to vehicle (DMSO) or UK-5099 (10 μ M for human PDAC, 25 μ M for murine PDAC) in DMEM supplemented with 1mM L-alanine. Data are represented as percentage relative to vehicle. Error bars depict s.d. of three technical replicate wells from one independent experiment. **(C)** Alanine uptake or secretion flux in a panel of human and mouse PDAC and hPSC#1 cultured in DMEM supplemented with 1mM L-alanine and either vehicle or UK-5099. Extracellular accumulation (+, secretion) or depletion (-, uptake) was measured in conditioned media over 24-72 hours and normalized to the viable cell density over the time course. Error bars depict s.d. of ≥ 3 technical replicate wells from 1-2 independent experiments normalized to growth of surrogate wells. Flux data plotted comparing data depicted Fig. 1A and 1G. **(D)** Lactate M+3 labeling normalized to alanine labeling (M+3) in PDAC cells in response to vehicle (DMSO) or UK-5099 cultured in DMEM supplemented with 1mM $^{13}\text{C}_3$ -alanine. Error bars depict s.d. of three technical replicates. Significance determined with two-way ANOVA using Sidak's multiple comparisons test in **B, D**. ** p-val < 0.01, *** p-val < 0.001.

Supplementary Fig. S4. Differential protein expression, including metabolic and transporter proteins, in PDAC and non-malignant pancreatic cell lines. (A) Principal component analysis (PCA) on whole proteome (*left panel*), metabolism proteins (*middle panel*), and 'SLC' transporter proteins (*right panel*) expressed in PDAC (PANC1, CAPAN-I, HPAC) and non-malignant pancreatic (HPNE, hPSC#1) cell lines. **(B)** Relative protein expression across panel of non-malignant pancreatic and PDAC cell lines quantified by summing reporter ion counts of peptide-spectral matches for SLC1A5, SLC17A5, and SLC6A6. SLC1A5, SLC17A5, and SLC6A6 were excluded as candidates due to differential expression in a single cell line. Two tandem mass tag-labeled biological replicates for each cell line. **(C)** Immunoblot of deglycosylated (PNGaseF) SLC38A2, SLC1A4, N/K-ATPase, and actin in whole cell lysates (20 μ g) collected from hPSC#1 and PANC1. Representative immunoblot depicted of five independent immunoblots. **(D)** Immunoblot of deglycosylated (PNGaseF) SLC38A2, N/K-ATPase, and actin in hPSC#1 and a panel of human PDAC cell lines. Representative immunoblot depicted of three independent immunoblots.

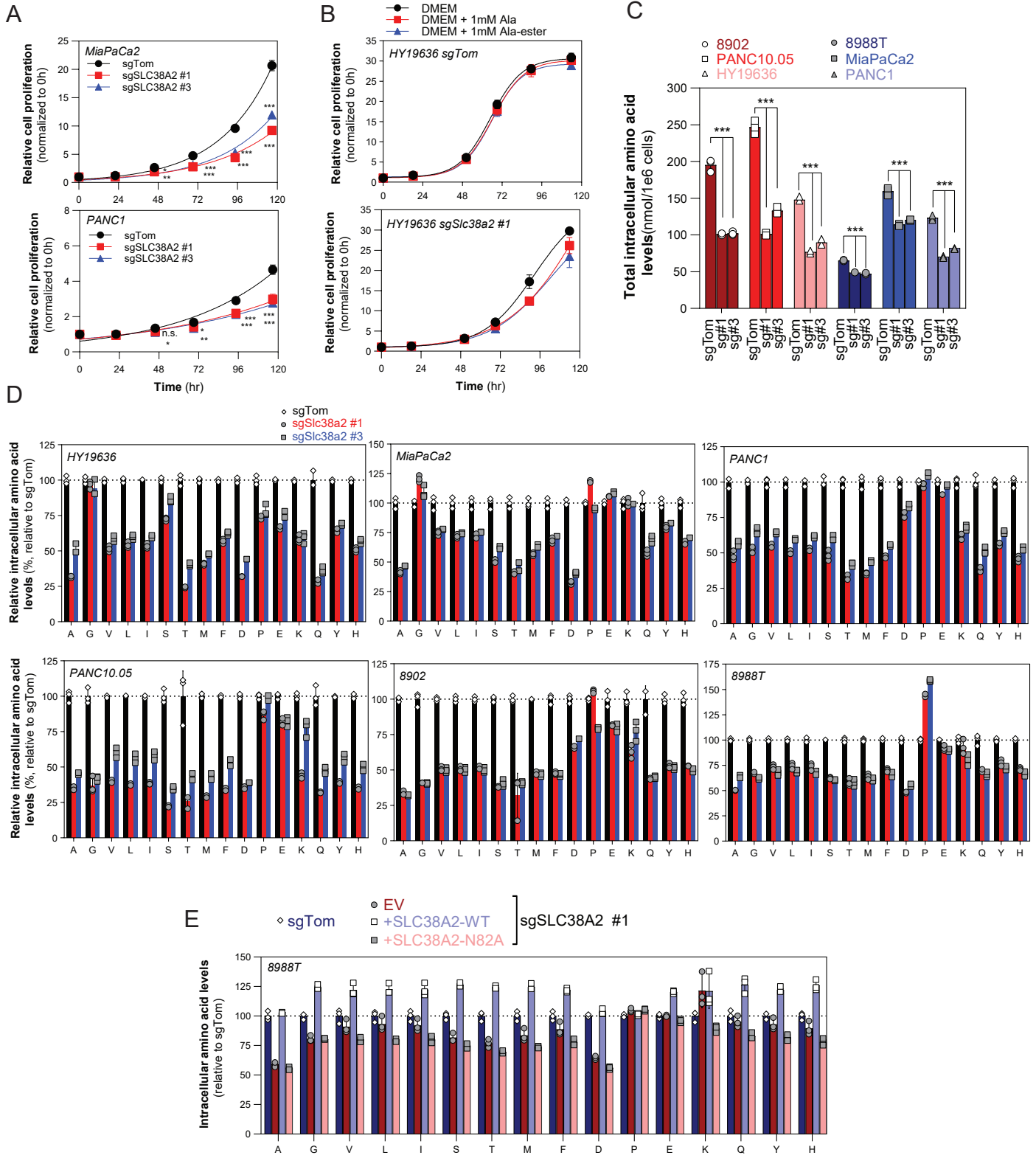
Supplementary Figure 5



Supplementary Fig. S5. SLC38A2 is necessary for concentrative alanine influx in PDAC.

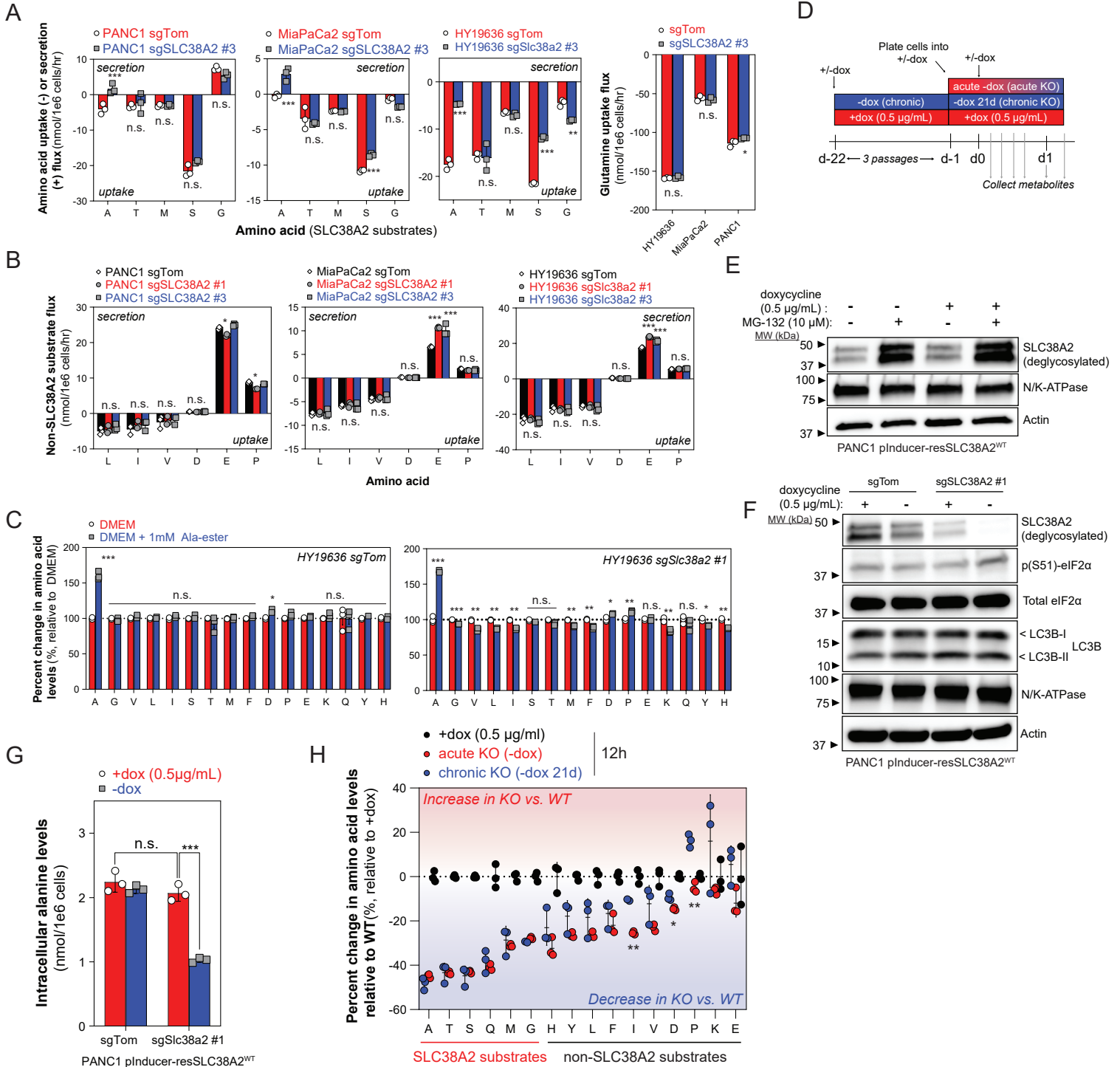
(A) Immunoblot of deglycosylated SLC38A2 and N/K-ATPase in whole cell lysates (20 μ g) extracted from pooled SLC38A2 knockout (sgSLC38A2 #1, #3) or control (sgTom) HY19636, MiaPaCa2, and PANC1 cells. Representative immunoblot depicted of three independent immunoblots. **(B)** Representative PDAC cell lines used for loss-of-function studies. PANC1 cells have low alanine demand relative to MiaPaCa2 and HY19636. Alanine demand quantified by treating cells with UK-5099 and quantifying alanine uptake in DMEM supplemented with 1mM L-alanine for 24 hours. Data plotted from Fig. 1G to compare HY19636, MiaPaCa2, and PANC1 alanine demands. **(C)** Immunoblot of deglycosylated SLC38A2, non-deglycosylated SLC38A2, and actin in whole cell lysates (20 μ g) extracted from 8988T control (sgTom), parental SLC38A2-deficient (sgSLC38A2 #1, -), and SLC38A2-deficient cells ectopically expressing empty vector (EV), sgRNA-resistant SLC38A2 (+SNAT2^{WT}), or mutant SLC38A2 incapable of binding to sodium (+SNAT2^{N82A}). Ectopically expressed SLC38A2 cDNAs, including non-functional mutant, are capable of forming mature protein evidenced by glycosylation capacity (*lower panel*). **(D)** Intracellular alanine levels in 8988T control (sgTom), SLC38A2-deficient (sgSLC38A2 #1; EV, SNAT2^{N82A}), and cDNA rescued (sgSLC38A2 #1; SNAT2^{WT}) cells cultured in DMEM (*left panel*) or DMEM supplemented with 1mM L-alanine (*right panel*) for 24 hours. Error bars depict s.d. of three technical replicate wells normalized to cell counts of surrogate wells. **(E)** Alanine carbon contribution to TCA cycle intermediates in SLC38A2-deficient (sgSLC38A2 #1, #3) or control (sgTom) HY19636, MiaPaCa2, and PANC1 cells cultured in DMEM supplemented with 1mM ¹³C₃-alanine for 1 hour. Error bars depict s.d. of three technical replicate wells per condition. **(F)** Intracellular alanine levels in SLC38A2-deficient (sgSlc38a2 #1) or control (sgTom) HY19636 cells cultured in DMEM or DMEM supplemented with 1mM of either L-alanine or L-alanine tert-butyl ester for 24 hours. Error bars depict s.d. of three technical replicate wells per condition normalized to cell counts of surrogate wells. Significance determined by two-way ANOVA using Sidak's multiple comparisons test in **D**, **E**, and **F**. n.s. p-val \geq 0.05, * p-val < 0.05, ** p-val < 0.01, *** p-val < 0.001.

Supplementary Figure 6



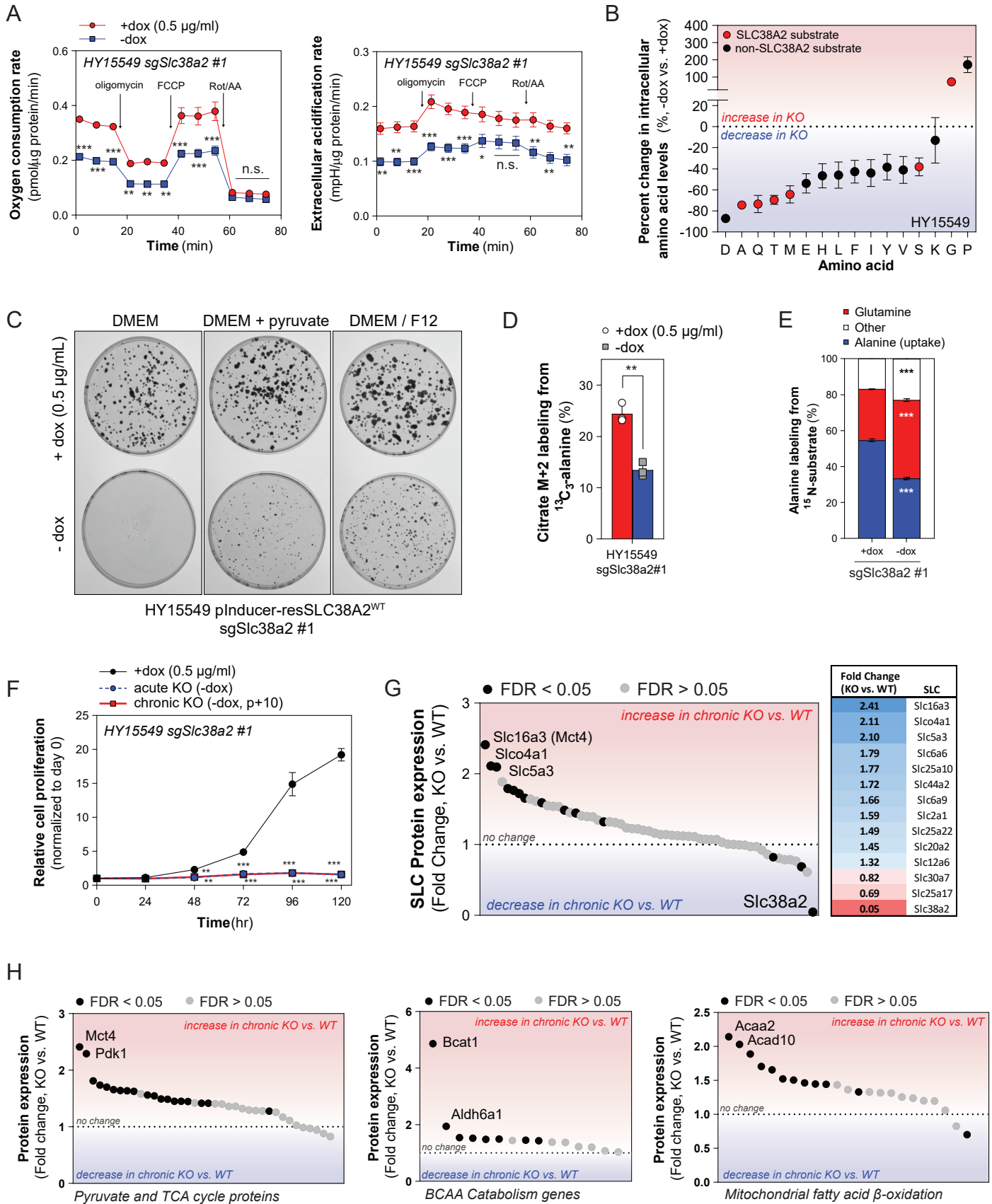
Supplementary Fig. S6. SLC38A2 loss in PDAC causes a metabolic crisis leading to decreased proliferative and clonogenic capacity. **(A)** Cell proliferation of control (sgTom) and SLC38A2-deficient (sgSLC38A2 #1, #3) MiaPaCa2 and PANC1 cells cultured in DMEM over five days. Data are plotted as cell proliferation relative to day 0 collected after cell attachment. Error bars depict s.d. of four technical replicate wells for each time point; representative data depicted from $n \geq 2$ independent experiments. Curves represent fitted exponential growth rates. **(B)** Cell proliferation of control (sgTom) and SLC38A2-deficient (sgSlc38a2 #1) HY19636 cells cultured in DMEM or DMEM supplemented with 1mM L-alanine or L-alanine tert-butyl ester over five days. Data are plotted as cell proliferation relative to day 0 collected after cell attachment. Error bars depict s.d. of four technical replicate wells for each time point. Curves represent fitted logarithmic growth rates. **(C)** Total intracellular amino acid levels normalized to 1×10^6 cells in SLC38A2-deficient (sgSLC38A2 #1, #3) or control (sgTom) 8902, PANC10.05, HY19636, 8988T, MiaPaCa2, or PANC1 cells cultured in DMEM for 24 hours. Error bars depict s.d. of three technical replicate wells per condition. **(D)** Amino acid composition relative to control (sgTom) cells in SLC38A2-deficient (sgSLC38A2 #1, #3) HY19636, MiaPaCa2, PANC1, PANC10.05, 8902, and 8988T cells cultured in DMEM for 24 hours. Panels are labeled with corresponding cell line and error bars depict s.d. of three technical replicate wells per condition. Plotted raw data used to calculate the percent change in amino acid levels plotted in Fig. 3D for sgSLC38A2 #1; also includes raw data for sgSLC38A2 #3. **(E)** Amino acid composition in 8988T control (sgTom), SLC38A2-deficient (sgSLC38A2 #1; EV, SNAT2^{N82A}), and cDNA rescued (sgSLC38A2 #1; SNAT2^{WT}) cells cultured in DMEM for 24 hours. Individual amino acid levels are normalized to control (sgTom) cells. Error bars depict s.d. of three technical replicate wells. Significance determined by two-way ANOVA using Dunnett's multiple comparisons test in **A**, **C**, **D**, and **E**. n.s. $p\text{-val} \geq 0.05$, * $p\text{-val} < 0.05$, ** $p\text{-val} < 0.01$, *** $p\text{-val} < 0.001$.

Supplementary Figure 7



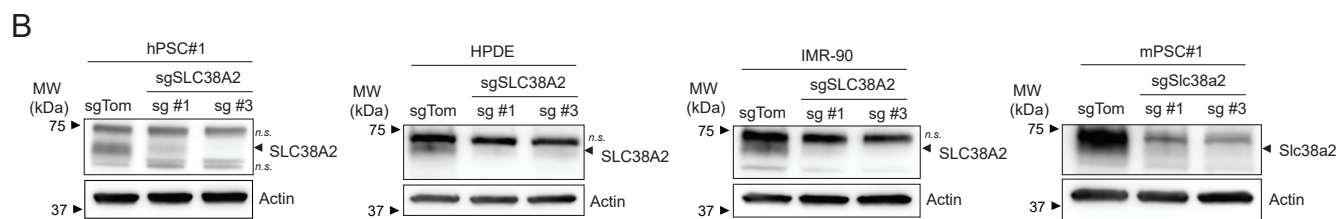
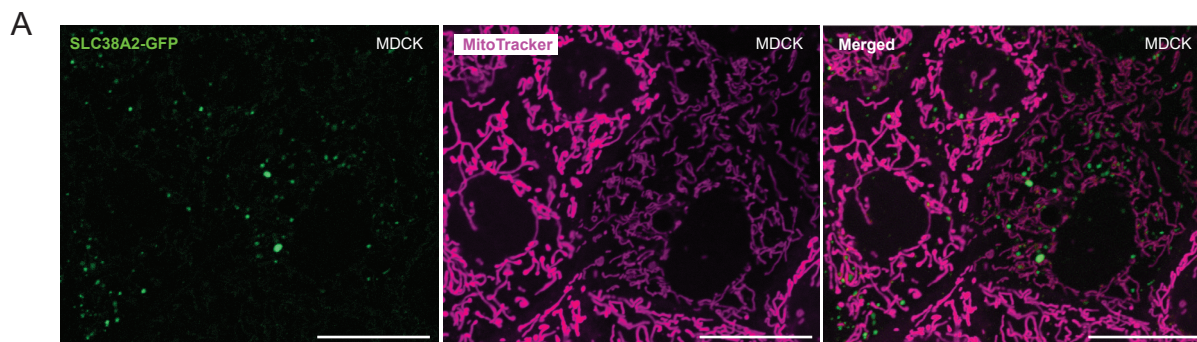
Supplementary Fig. S7. Reduced capacity to influx alanine drives amino acid crisis in SLC38A2-deficient PDAC cells. (A) Alanine and other SLC38A2 substrate (e.g. threonine, methionine, serine, glycine, glutamine) uptake and secretion fluxes in SLC38A2-deficient (sgSLC38A2 #3) and control (sgTom) PANC1, MiaPaCa2, and HY19636 cells cultured in basal DMEM. Data from same experiment as Fig. 2D, 3E, and 3F plotted to compare control (sgTom) to sgSLC38A2 #3. (B) Non-SLC38A2 substrate (e.g. leucine, isoleucine, valine, aspartate, glutamate, proline) uptake and secretion fluxes in SLC38A2-deficient (sgSLC38A2 #1, #3) and control (sgTom) PANC1, MiaPaCa2, and HY19636 cells cultured in basal DMEM. For A and B, Extracellular accumulation (+, secretion) or depletion (-, uptake) was measured in conditioned media over 24 hours and normalized to the viable cell density over the time course. (C) Percent change in intracellular amino acids in control (sgTom, *left panel*) and SLC38A2-deficient (sgSlc38a2 #1, *right panel*) HY19636 cells cultured in DMEM of DMEM supplemented with 1mM of L-alanine tert-butyl ester for 4 hours. Data presented as a percent change for each amino acid relative to DMEM conditions. Cell-permeable L-alanine tert-butyl ester failed to rescue the amino acid defect in SLC38A2-deficient cells as evidenced by failure to increase amino acid levels relative to DMEM. Error bars in A, B, and C depict s.d. of ≥ 3 technical replicate wells normalized to cell growth of surrogate wells. (D) Diagram depicting generation of dox-inducible SLC38A2 cells lacking endogenous SLC38A2 locus deleted via CRISPR/Cas9. SLC38A2-expressing cells were maintained in doxycycline (0.5 $\mu\text{g}/\text{mL}$). To generate chronic SLC38A2-null cells, doxycycline was washed out and cells were cultured in basal DMEM (-dox) for 21 days. For metabolomics experiments, doxycycline was acutely withdrawn from SLC38A2-expressing cells and metabolites were collected over the course of 32 hours and compared to metabolite levels extracted from SLC38A2-expressing cells (+dox) or chronic SLC38A2-deficient cells (chronic KO). (E) Immunoblot of deglycosylated (PNGaseF) SLC38A2, N/K-ATPase, and actin in whole cell lysates (20 μg) extracted from PANC1 pInducer-resSLC38A2^{WT} cells cultured in DMEM supplemented \pm doxycycline (0.5 $\mu\text{g}/\text{mL}$) for 24 hours prior to treatment with vehicle (DMSO) or proteasomal inhibitor MG-132 (10 μM) for 16 hours. (F) Immunoblot of deglycosylated (PNGaseF) SLC38A2, p(S51)-eIF2 α , total eIF2 α , LC3B, N/K-ATPase, and actin in whole cell lysates (20 μg) extracted from PANC1 pInducer-resSLC38A2^{WT} control (sgTom) and SLC38A2-deficient (sgSLC38A2 #1) cells cultured in presence of doxycycline (0.5 $\mu\text{g}/\text{mL}$) or after wash-out of doxycycline for 24 hours. (G) Intracellular alanine levels normalized to 1×10^6 cells in PANC1 pInducer-resSLC38A2^{WT} control (sgTom) and SLC38A2-deficient (sgSLC38A2 #1) cells cultured in presence of doxycycline (0.5 $\mu\text{g}/\text{mL}$) or after wash-out of doxycycline for 24 hours. Error bars depict s.d. of three technical replicate wells normalized to cell counts of surrogate wells. (H) Percent increase (+) or decrease (-) in intracellular amino acids in acute SLC38A2-deficient (acute KO, -dox for 12 hours) and chronic SLC38A2-deficient (chronic KO, -dox) compared to SLC38A2-expressing (WT, +dox; set to 0%) PANC1 pInducer-resSLC38A2^{WT} cells. Data are presented as a percent change relative to SLC38A2-expressing cells (WT, +dox). Error bars depict s.d. of three technical replicate wells normalized to cell counts of surrogate wells. Data are included in Fig. 3G and 3H (alanine and aspartate) plotted to compare acute KO and chronic KO to +dox condition at 12-hour time point. Statistics determined by two-way ANOVA using Sidak's multiple comparisons test in A, G; two-way ANOVA using Dunnett's multiple comparisons test in B; t-test in C, H. n.s. p-val \geq 0.05, * p-val < 0.05, ** p-val < 0.01, *** p-val < 0.001.

Supplementary Figure 8



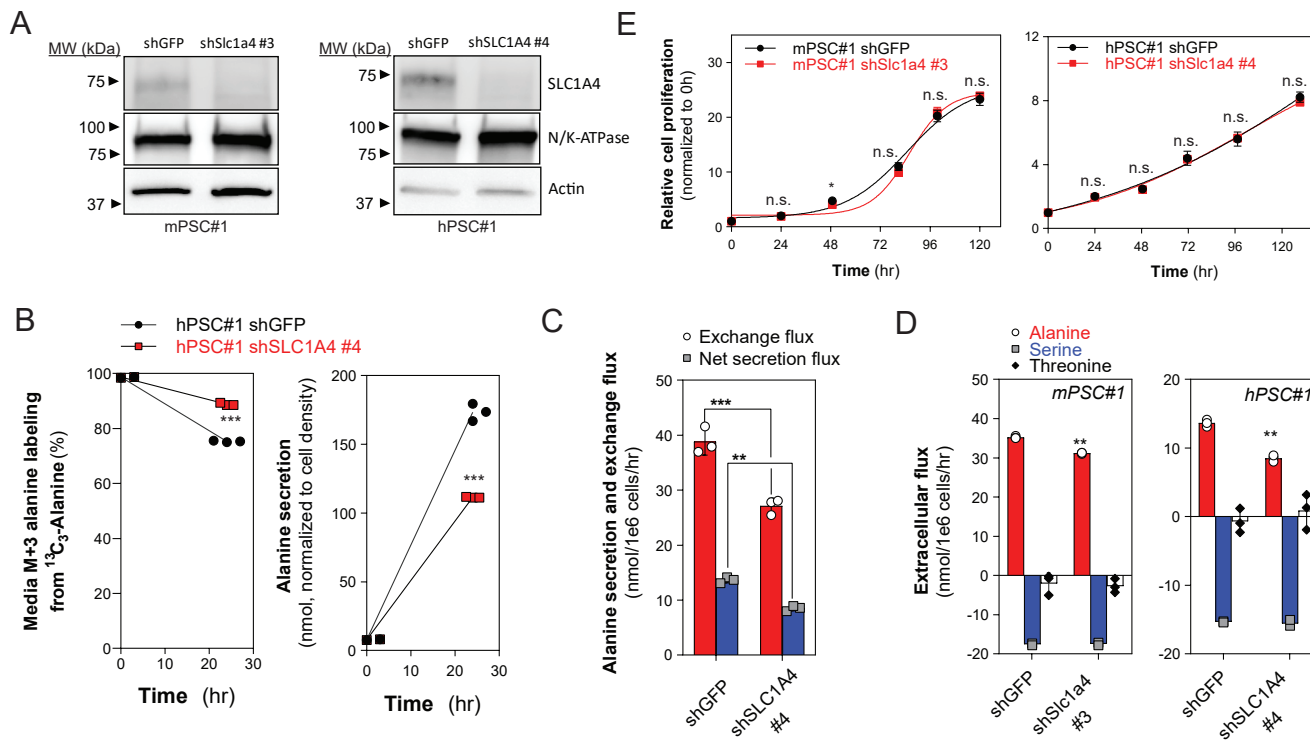
Supplementary Fig. S8. SLC38A2 deficiency causes compartmentalized redox crisis and incomplete metabolic compensation. **(A)** Oxygen consumption rate (OCR, *left panel*) and extracellular acidification rate (ECAR, *right panel*) in clonally derived HY15549 Slc38a2-deficient (sgSlc38a2 #1) cells expressing doxycycline-inducible sgRNA-resistant SLC38A2 cDNA. Cells were cultured in the presence of doxycycline (+dox, 0.5 μ g/ml) or after overnight washout (-dox) prior to analysis of OCR and ECAR. Error bars depict s.e.m. of four representative independent experiments consisting of ≥ 10 technical replicate wells for each condition and experiment. Raw data plotted from same experiments used to calculate percent change in OCR and ECAR in Fig. 4D. **(B)** Increase (+) and decrease (-) in intracellular amino acid levels in SLC38A2-deficient HY15549 cells (-dox) relative to control cells (+dox). All amino acid levels were normalized to cell number (1×10^6 cells) prior to comparison to control (+dox); SLC38A2 substrates are indicated by red circles. Error bars depict s.e.m. of ≥ 3 technical replicate wells from four independent experiments. Dotted line indicates no change and positive and negative values indicate an increase and decrease in amino acid levels in SLC38A2-deficient ("KO") cells relative to control ("WT") cells, respectively. **(C)** Representative plates from clonogenic assay of clonally derived Slc38a2-deficient (sgSlc38a2 #1) HY15549 cells cultured in DMEM, DMEM supplemented with 1mM pyruvate, or DMEM/F12 (50:50) +dox or -dox over 7-10 days. Representative clonogenic plates selected from ≥ 3 independent experiments of three technical replicate plates for each condition. Same representative control (DMEM) clonogenic plates as in Fig. 4C; used here to compare control to representative metabolite rescue plates. **(D)** Alanine carbon contribution to citrate in SLC38A2-deficient (-dox) or control (+dox) HY15549 cells cultured in DMEM supplemented with 1mM $^{13}\text{C}_3$ -alanine for 1 hour. Error bars depict s.d. of three technical replicate wells per condition. **(E)** Intracellular alanine labeling in SLC38A2-deficient (-dox) or control (+dox) HY15549 cells cultured in DMEM supplemented with either 1mM ^{15}N -alanine and 4mM L-glutamine or 1mM L-alanine and 4mM α - ^{15}N -glutamine for 24 hours. Error bars depict s.d. of three technical replicate wells per condition. Raw alanine labeling data from same experiment used to calculate percent change in labeling from ^{15}N -alanine and glutamine in Fig. 4G. **(F)** Cell proliferation of clonally derived Slc38a2-deficient (sgSlc38a2 #1) HY15549 cell line cultured over five days in either control conditions (+dox), after acute dox withdrawal (acute KO, -dox), or chronic dox withdrawal (chronic KO, -dox). Chronic KO cells were generated by culturing isogenic clonally derived HY15549 cells in basal DMEM (-dox) for 10 passages (p+10). Data are plotted as cell proliferation relative to day 0 collected after cell attachment. Error bars depict s.e.m. of ≥ 3 independent experiments of four technical replicate wells for each time point. **(G)** Differential SLC protein expression in chronic KO (-dox, 10 passages) or SLC38A2-expressing (+dox) HY15549 cells. Up-regulated SLCs (FC > 1) and down-regulated SLCs (FC < 1) in chronic SLC38A2 KO cells; significantly expressed SLCs indicated by black circles (*left panel*, FDR < 0.05) and indicated with fold changes in table (*right panel*). **(H)** Differential protein expression in chronic KO (-dox, 10 passages) or SLC38A2-expressing (+dox) HY15549 cells involved in pyruvate and TCA cycle (*left panel*), branched chain amino acid (BCAA) catabolism (*middle panel*), and mitochondrial fatty acid β -oxidation (*right panel*) from Gene Set Enrichment Analysis (GSEA). Significantly differential expressed proteins indicated by black circles (FDR < 0.05). Significance determined by two-way ANOVA using Sidak's multiple comparisons test in **A**, **E**, and **F**; Two-tailed t-test in **D**; multiple hypothesis testing using Benjamini-Hochberg method in **G**, **H**. n.s. p-val ≥ 0.05 , * p-val < 0.05 , ** p-val < 0.01 , *** p-val < 0.001 .

Supplementary Figure 9



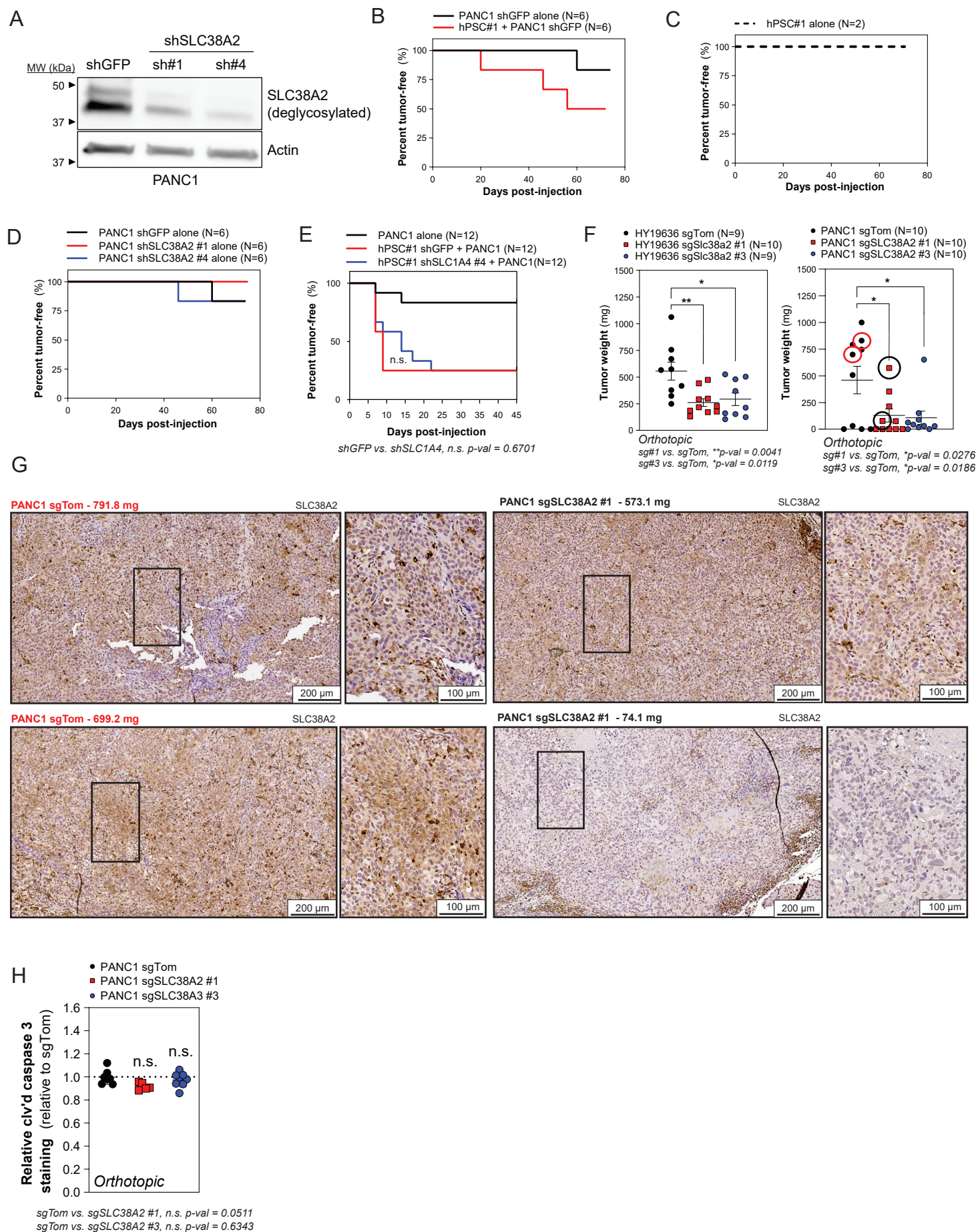
Supplementary Fig. S9. Differential SLC38A2 localization in PDAC and non-malignant cells. (A) Representative live cell images of MDCK cells transiently transfected with 3 μ g of SLC38A2-GFP (green) overnight. Live cells were imaged using MitoTracker. Representative fields containing 1-2 cells from ≥ 5 fields from ≥ 3 independent experiments. Scale bars are indicated in each panel; 5 μ m. (B) Representative immunoblot of SLC38A2 and Actin in whole cell lysates (30 μ g) extracted from pooled SLC38A2 knockout (sgSLC38A2 #1, #3) or control (sgTom) hPSC#1, HPDE, IMR-90, and mPSC#1 cells. Representative immunoblot depicted of two independent immunoblots. n.s. indicates non-specific band; arrow indicates glycosylated SLC38A2 protein.

Supplementary Figure 10



Supplementary Fig. S10. SLC1A4 cooperates with another passive transporter in pancreatic stellate cells to facilitate alanine secretion and exchange. (A) Immunoblot of SLC1A4, N/K-ATPase, and actin in whole cell lysates (30 µg) extracted from hPSC#1 (shGFP, shSLC1A4 #4) and mPSC#1 (shGFP, shSlc1a3 #3) cultured in DMEM. **(B)** Extracellular alanine label (M+3) dilution with unlabeled (M+0) alanine in SLC1A4 knockdown or control (shGFP) hPSC#1 cells cultured in DMEM supplemented with 1mM ¹³C₃-alanine for 24 hours (*left panel*). Net alanine secretion normalized to relative cell growth from control (shGFP) and SLC1A4 knockdown hPSC#1 cells cultured in DMEM for 24 hours (*right panel*). Error bars depict s.d. of three technical replicate wells normalized to cell counts of surrogate wells. Raw data used to calculate net alanine secretion flux and exchange flux plotted in **C** and **D**. **(C)** Alanine secretion or exchange flux in SLC1A4 knockdown or control (shGFP) hPSC#1 cells cultured in DMEM or DMEM supplemented with 1mM ¹³C₃-alanine. Net secretion flux calculated from molar secretion normalized to cell density over time. Exchange flux calculated from carbon turnover rate calculated from molar ¹³C₃-alanine dilution normalized to cell density over time. Error bars depict s.d. of ≥3 technical replicate wells normalized to cell counts of surrogate wells. **(D)** Extracellular flux of SLC1A4 substrates including alanine, serine, and threonine in SLC1A4 knockdown and control (shGFP) mPSC#1 (*left panel*) and hPSC#1 (*right panel*) cells cultured in DMEM for 24 hours. Error bars depict s.d. of ≥3 technical replicate wells normalized to cell counts of surrogate wells. **(E)** Cell proliferation relative to day 0 in SLC1A4 knockdown and control (shGFP) human and mouse stellate cell lines cultured in DMEM over five days. Error bars depict s.d. of four technical replicate wells per time point. Significance determined by two-way ANOVA using Sidak's multiple comparisons test in **C**, **D**; two-tailed t-test in **B**, **E**. n.s. p-val ≥ 0.05, * p-val < 0.05, ** p-val < 0.01, *** p-val < 0.001.

Supplementary Figure 11



Supplementary Fig. S11. SLC38A2 is vital for tumor initiation and maintenance. (A) Immunoblot of deglycosylated (PNGaseF) SLC38A2 and actin in whole cell lysates (20 μ g) extracted from SLC38A2 knockdown (shSLC38A2 #1, #4) and control (shGFP) PANC1 cells immediately prior to xenograft experiments. **(B)** Tumor initiation was enhanced when control (shGFP) PANC1 cells (2×10^5) were co-injected with hPSC#1 cells (1×10^6) in a subcutaneous xenograft model. **(C)** Stellate cells injected alone (1×10^6) did not form tumors. **(D)** SLC38A2 knockdown (shSLC38A2 #1, #4) and control (shGFP) PANC1 cells (2×10^5) injected alone rarely formed tumors in a subcutaneous xenograft model. **(E)** Both control (shGFP) and SLC1A4 knockdown (shSLC1A4 #4) hPSC#1 cells (1×10^6) co-injected with PANC1 cells (2×10^5) promoted tumor initiation in a subcutaneous xenograft model. **(B to E)** Mice were monitored bi-weekly by caliper measurement, and tumors were considered initiated if length and width were both ≥ 1 mm. Each injected flank was considered a possible tumor when calculating percent tumor-free. **(F)** Knockout of SLC38A2 significantly reduced tumor burden in HY19636 and PANC1 orthotopic syngeneic allograft and xenograft models, respectively. HY19636 (2.5×10^4) or PANC1 (5×10^5) control (sgTom) or pooled SLC38A2-deficient (sgSLC38A2 #1, #3) cells were injected orthotopically, and tumors were weighed following resection after 27 days (HY19636) or 63 days (PANC1). Error bars depict s.e.m. of tumors resected from 9-10 mice. Circles indicate tumors submitted for immunohistochemical analysis of SLC38A2 expression status. **(G)** Immunohistochemical staining of SLC38A2 in representative control (sgTom, *left panels*) and large “escaper” or small tumors from SLC38A2-deficient cells (sgSLC38A2 #1, *right panels*) indicated with circles in **F**. Positive SLC38A2 staining observed in large tumors derived from pooled CRISPR/Cas9 SLC38A2 knockout, suggesting escape of SLC38A2-expressing cells. Very low, to no staining for SLC38A2 observed in small SLC38A2-deficient tumors confirming specificity of antibody for immunohistochemistry. Representative images from two independent experiments; scale bars indicated in each panel. **(H)** Quantification by optical density of DAB staining of cleaved caspase 3 in orthotopic control (sgTom) and SLC38A2-deficient (sgSLC38A2 #1, #3) tumors. Significance determined by log-rank Mantel-Cox test in **E**; one-way ANOVA using Dunnett’s multiple comparisons test in **F**, **H**. n.s. p-val ≥ 0.05 , * p-val < 0.05 , ** p-val < 0.01 , *** p-val < 0.001 .

Supplementary Table S1. Differentially expressed transporters between hPSC#1 and PANC1 cells.

SLC protein	FC	p-val
SLC8A1	11.320	0.032
SLC39A8	8.896	0.001
SLC27A2	4.439	0.023
SLC44A1	3.593	0.012
SLC2A3	2.927	0.002
SLC9A3R1	2.771	0.026
SLC44A2	2.583	0.002
SLC2A1	2.519	0.007
SLC1A4	2.490	0.042
SLC27A1	2.313	0.025
SLC1A5	2.213	0.001
SLC30A9	2.134	0.001
SLC22A18	18.320	0.004
SLC12A7	11.024	0.016
SLC26A2	7.795	0.001
SLC25A21	6.905	0.001
SLCO4A1	6.859	0.019
SLC46A1	6.322	0.002
SLC25A13	5.786	0.003
SLC25A22	5.514	0.002
SLC39A1	5.448	0.039
SLC5A3	5.282	0.012
SLC6A6	4.641	0.020
SLC11A2	3.731	0.032
SLC17A5	3.577	0.011
SLC38A2	3.461	0.007
SLC30A5	3.415	0.015
SLC30A1	3.412	0.002
SLC35F6	3.205	0.004
SLC25A40	2.803	0.002
SLC15A4	2.792	0.031
SLC30A6	2.783	0.006
SLC29A1	2.572	0.001
SLC25A35	2.496	0.031
SLC25A1	2.391	0.003
SLC25A20	2.231	0.000
SLC25A17	2.222	0.015
SLC9A3R2	2.193	0.006
SLC9A3R2	2.154	0.011
SLC25A12	2.046	0.043

Higher in hPSC#1
Higher in PANC1